

Review

# Molecular Structures and Second-Order Nonlinear Optical Properties of Ionic Organic Crystal Materials

Xiu Liu, Zhou Yang \*, Dong Wang and Hui Cao

Beijing Key Laboratory of Function Materials for Molecule & Structure Construction, School of Materials Science and Engineering, University of Science and Technology Beijing, Beijing 100083, China; liuxiu0206@163.com (X.L.); wangdong@ustb.edu.cn (D.W.); caohui@mater.ustb.edu.cn (H.C.)

\* Correspondence: yangz@ustb.edu.cn; Tel.: +86-10-62333759

Academic Editor: Helmut Cölfen

Received: 1 September 2016; Accepted: 25 November 2016; Published: 14 December 2016

**Abstract:** In recent years, there has been extensive research and continuous development on second-order nonlinear optical (NLO) crystal materials due to their potential applications in telecommunications, THz imaging and spectroscopy, optical information processing, and optical data storage. Recent progress in second-order NLO ionic organic crystal materials is reviewed in this article. Research has shown that the second-order nonlinear optical properties of organic crystal materials are closely related to their molecular structures. The basic structures of ionic organic conjugated molecules with excellent nonlinear optical properties are summarized. The effects of molecular structure, for example, conjugated  $\pi$  electron systems, electronic properties of donor-acceptor groups, and different counter-anion effects on second order NLO properties and crystal packing are studied.

**Keywords:** second-order nonlinear optical material; ionic organic crystal; D- $\pi$ -A conjugated molecule

## 1. Introduction

There has been considerable interest in organic nonlinear optical (NLO) materials with large second-order optical nonlinearities due to their attractive potential applications in optical frequency conversion, integrated photonics, high-speed information processing, and THz wave generation and detection [1–3]. These materials have low dispersion of their dielectric constants (refractive index) and nonlinear optical susceptibility from direct current (low frequency) to the optical frequency range, because of their dominant electronic contribution to linear and nonlinear optical material polarizability [4–7]. This permits an ultra-fast polarizability response time compared to inorganic materials, whose dominant response usually comes from intrinsically slower acoustic and optical lattice vibrations. Additionally, the nonlinear optical figures of merit of organic materials may be several orders of magnitude higher than those of their inorganic counterparts and they have almost unlimited design possibilities [8,9]. All these advantages make organic NLO materials extremely attractive for the above mentioned applications. It has become an important research focus to design and synthesize new organic NLO materials with excellent performance. Among them, single crystals are one of the most attractive materials owing to their typically large macroscopic nonlinearities, high packing densities, and excellent long-term orientational and photochemical stabilities, as well as their superior optical quality.

Second harmonic generation (SHG) is a nonlinear optical process, in which photons with the same frequency interacting with a nonlinear material are effectively combined to generate new photons with twice the energy, and therefore twice the frequency and half the wavelength of the initial photons [10]. To obtain large second-order NLO effects, it is necessary to investigate both microscopic and macroscopic NLO properties of organic materials. On the microscopic level, molecular nonlinearity is determined by the molecular structures and their electronic properties. In general,

dipolar molecule units containing highly delocalized conjugated systems and strong electron acceptors ( $-\text{NO}_2$ ,  $-\text{COOH}$ ,  $-\text{SO}_3\text{H}$ ,  $-\text{CN}$ , etc.) and electron donors ( $-\text{NR}_2$ ,  $-\text{OR}$ , etc.) lead to large molecular first hyperpolarizabilities ( $\beta$ ). In addition to a large first-order hyperpolarizability of the molecules, the macroscopic second order susceptibilities ( $\chi^{(2)}$ ) are strongly dependent on the relative alignment of the  $\pi$ -conjugated chromophores [11]. However, about 75% of the nonchiral organic chromophores crystallize centrosymmetrically and thereby exhibit no macroscopic second-order optical nonlinearity. The non-centrosymmetric arrangement of the chromophores in the crystalline lattice is one of the most crucial issues in developing ideal and highly successful second-order NLO crystalline materials [12]. There have been several approaches used to factitiously achieve non-centrosymmetry. The utilization of strong coulomb interactions, for example, the crystallization of ionic salts [13] to overcome the symmetry problem has been proved to be a simple and efficient strategy to obtain materials with large  $\chi^{(2)}$ .

Inside D- $\pi$ -A conjugated organic ionic species, the cation is the main source of nonlinear properties, whereas the counter-anion is used to adjust the crystal packing through coulombic interactions [14–17]. The suitable combination of cation and counter-anion would lead to high second-order optical nonlinearity. Stilbazolium organic salt occupy an important position in the field of nonlinear optics owing to their larger nonlinear optical effect. Especially, 4-*N,N*-dimethylamino-4-*N*,-methyl-stilbazolium tosylate (DAST); this is one of the best NLO crystals with large second-order nonlinear optical susceptibilities  $\chi_{111}^{(2)} = 2020 \pm 200$  pm/V at 1.3  $\mu\text{m}$  and  $\chi_{111}^{(2)} = 420 \pm 110$  pm/V at 1.9  $\mu\text{m}$  due to the appropriate orientation of the chromophores in the crystal [18–20]. DAST consists of a positively charged nonlinear optical chromophore stilbazolium and a negatively charged tosylate anion. However, the upper limits of theoretical calculated macroscopic susceptibilities for DAST are by far not yet achieved [21]. Besides, the growth of highly nonlinear optical quality bulk or thin films of DAST single crystals still remains an urgent challenge. It usually takes one or two months to grow high-quality and large-size DAST crystals, and the growth process requests high precision in temperature fluctuations. Therefore it is desirable to develop new organic crystals with larger NLO properties and better crystal growth abilities compared with those of DAST [22].

## 2. Physical Explanations and NLO Measurement Method

### 2.1. Physical Explanations

A laser is a source of light and the light emitted by a laser has a very high degree of collimation and coherence. The light of a laser beam is highly monochromatic and can be focused to a minimum spot size on a material. Therefore, a focused laser beam can provide a high power per unit area. The laser light can stimulate atomic or molecular systems to produce transition and release the stored energy also as light. Therefore what we have is a process of controlling the light by light in the atomic or molecular system. When the electromagnetic field of a laser beam is illuminated on an atom or a molecule, it induces electrical polarization that gives rise to many of the unusual and interesting properties that are optically nonlinear [23]. A relationship between the polarization  $P$  induced in a molecule and the applied electric field  $E$  can be written by

$$P = \varepsilon_0 \alpha E + \varepsilon_0 \beta E^2 + \varepsilon_0 \gamma E^3 + \dots \quad (1)$$

where  $\varepsilon_0$  is the vacuum dielectric constant,  $\alpha$  is the linear polarization,  $\beta$  and  $\gamma$  are the first and second hyperpolarizability, respectively. Furthermore, the even order tensor  $\beta$ , responsible for second-order NLO effects (for example SHG), requests non-centrosymmetric molecular structure and crystal packing.

It is also well established that the macroscopic polarization of a bulk material under an applied strong electric field can be regarded as an averaged sum of the individual molecular polarizations [24]:

$$P = \chi_{\text{IJK}}^{(1)} E + \chi_{\text{IJK}}^{(2)} E^2 + \chi_{\text{IJK}}^{(3)} E^3 + \dots \quad (2)$$

where  $\chi_{IJK}^{(2)}$  and  $\chi_{IJK}^{(3)}$  are the second and third order susceptibility tensors, respectively.

The expected powder measurement efficiency of a novel crystal could be estimated in some ways through a mathematical model. Firstly, some reasonable assumptions were made for calculation. Any influence of the intermolecular interactions and any contribution of the counter-anion to the nonlinearity is not considered. To estimate suppose that the stilbazolium chromophore is essentially unidimensional, with only one leading component  $\beta$  of the first-hyperpolarizability tensor along the orientation of the long axis in chromophore. The susceptibility tensor  $\chi_{IJK}^{(2)}$  can be related to the microscopic first hyperpolarizabilities  $\beta_{ijk}$  using the oriented-gas model [25] as:

$$\chi_{IJK}^{(2)} = NF_{IJK}\beta_{IJK}^{\text{eff}} \quad (3)$$

where  $N$  is the number density of the chromophores,  $F_{IJK}$  is the correction factors due to intermolecular interactions, and  $\beta_{IJK}^{\text{eff}}$  is the effective hyperpolarizability of the crystalline system, which can be calculated by the following formula:

$$\beta_{IJK}^{\text{eff}} = \Sigma \cos\theta(I, i) \cdot \cos\theta(J, j) \cdot \cos\theta(K, k) \beta_{IJK} \quad (4)$$

Take DAST for example, the four chromophores in the unit cell are aligned along the  $3a + b$  and along the  $3a - b$  crystallographic vectors, and therefore make an angle of about  $\theta = 20^\circ$  with respect to the polar axis  $a$ . The effective hyperpolarizability of the unit cell in the crystal of DAST only depends on the following components:

$$\beta_{111}^{\text{eff}} = \beta \cos^3\theta = 0.83\beta \text{ and } \beta_{221}^{\text{eff}} = \beta_{212}^{\text{eff}} = \beta_{122}^{\text{eff}} = \beta \cos\theta \sin^2\theta = 0.11\beta. \quad (5)$$

The powder measurement efficiency depends on  $N$  and the squared effective  $\beta$  components, averaged over all possible orientations  $\langle (\beta^{\text{eff}})^2 \rangle$ . In case that only two effective components  $\beta_{111}^{\text{eff}}$  and  $\beta_{221}^{\text{eff}} = \beta_{212}^{\text{eff}} = \beta_{122}^{\text{eff}}$  are non-zero,  $\langle (\beta^{\text{eff}})^2 \rangle$  can be expressed as

$$\langle (\beta^{\text{eff}})^2 \rangle = \frac{1}{105} (19(\beta_{111}^{\text{eff}})^2 + 13\beta_{111}^{\text{eff}}\beta_{221}^{\text{eff}} + 44(\beta_{221}^{\text{eff}})^2), \quad (6)$$

which gives  $\langle (\beta^{\text{eff}})^2 \rangle_{\text{DAST}} = 0.14\beta^2$  for DAST [26].

## 2.2. NLO Measurement Method

### 2.2.1. Kurtz and Perry Powder Technique for SHG Efficiency

Kurtz and Perry powder technique [27] is a simple and quick experimental method which only requires the material in powder form for evaluating the SHG efficiency of nonlinear optical materials. Powders were made from single crystals using a Spex vibrating ball mill, and then graded using standard sieves. A laser beam of fundamental wave-length 1064 nm from a Q-switched Nd:YAG laser, 8 ns pulse width, with 10 Hz pulse rate was made to fall normally on the pre-packed microcapillary tube [28]. Second harmonic radiation generated by the randomly oriented microcrystals were focused by a lens and detected by the photomultiplier tube. The efficient responses for SHG mainly depend on the particle size, field-gain coefficient, the power of the fundamental beam, and the minimum beam waist [29].

### 2.2.2. Maker-Fringe Technique for Optical Tensor Element

The nonlinear optical tensor elements were tested by the standard Maker-fringe technique generalized for anisotropic absorbing materials. In order to avoid absorption of the generated second-harmonic wave, the experiment must be performed with a fundamental wavelength longer than twice the absorption edge of the sample. For example the measurement of the 4-*N,N*-dimethylamino-4'-*N'*-methyl-stilbazolium 2,4,6-trimethylbenzenesulfonate (DSTMS) [30], fundamental wavelength of 1907 nm generated by stimulated Raman scattering in pressurized

hydrogen gas was used, pumped by a Q-switched Nd:YAG laser operating at 1064 nm. A typical Maker-fringe data obtained by measuring the  $d_{111}$  element of DSTMS is demonstrated in Figure 1. With  $c$  plates of DSTMS the nonlinear optical susceptibility elements  $d_{111}$ ,  $d_{212}$ , and  $d_{122}$  could be measured by selecting the appropriate polarization of the fundamental and of the second harmonic waves. Quartz with  $d_{111} = 0.277$  pm/V at 1.9  $\mu\text{m}$  was chosen for the reference substance compared to the measurement. The nonlinear optical tensor element  $d_{111}$  is the largest due to the preferential alignment of the chromophores along the  $x_1$  axis of the DSTMS.

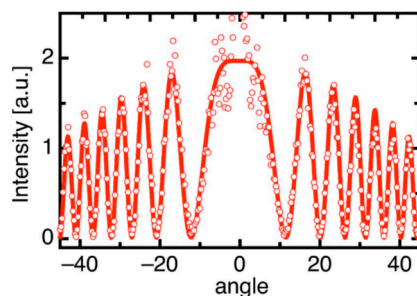


**Figure 1.** (Color online) Maker-fringe curve obtained by rotating a  $c$  plate 4- $N,N$ -dimethylamino-4'- $N'$ -methyl-stilbazolium 2,4,6-trimethylbenzenesulfonate (DSTMS) crystal around the dielectric  $x_1$  axis. The impinging fundamental beam at 1.9  $\mu\text{m}$  as well as the generated second-harmonic light at 0.95  $\mu\text{m}$  were  $s$  polarized [27].

### 3. Design of Second-Order NLO Organic Crystal Materials

#### 3.1. Design of Anionic Change

There has been intensive research and continuous development in second-order NLO organic crystal materials, aimed at obtaining new organic materials with large nonlinear, excellent ability of crystal growth, and high temperature and light stability. Variation of counter-ions in organic salts has been confirmed to be an easy and high-efficiency approach for creating crystals with large second-order NLO activity. Study has indicated that even very minor changes in the structures of the counter-anion play an important role in macroscopical lattice stacking [31]. Research on using different counter-anions to induce molecule arranging with the same cation of DAST has made some achievements [32–37]. Well-designed counter-anions are more likely to form non-centrosymmetric structures having even higher NLO properties than DAST. DAST derivatives (Figure 2) with ethyl-substituted cations were designed and synthesized by Okada et al. in the early years [38]. Counter anion exchange afforded several SHG active crystals even in ethyl-substituted derivatives. Among them, the crystal structure of (2d) belongs to the monoclinic space group  $P2_1$  with a polar  $b$ -axis. Crystal 1c gives an isomorphous crystal structure with DAST, it has excellent second-order nonlinear optical properties similar to that of DAST. Moreover, it can also be applied for terahertz-wave generation.

In the early years, study on the appeal of acid anion replacement of DAST tended to be more casual. Yang et al. investigated new stilbazolium salts which were grouped into three series with various kinds of counter anions [39]. Comparison of the experimental results (Figure 3) revealed that introducing especially long counter anions into stilbazolium derivatives does not only restrain the SHG activity but also influences the growth of single crystals. On the other hand, it is more probable to induce a non-centrosymmetric structure with higher SHG activity than that of DAST, while using a bulky counter anion compared to the tosylate of DAST, even a relatively bulk counter-anion may still lead to difficulty of nucleation of the compounds. For example, DSNS [34] (4- $N,N$ -dimethylamino-4'- $N'$ -methyl-stilbazolium 2-naphthalenesulfonate) was highlighted for its second-order nonlinearity, which is 50% higher than that of DAST at 1907 nm, but it is quite difficult to get its bulk single crystal. DSTMS [40] (4- $N,N$ -dimethylamino-4'- $N'$ -methyl-stilbazolium 2,4,6-trimethylbenzenesulfonate) with similar second-order susceptibilities with DAST possesses

better growth characteristics. A size of  $33 \times 33 \times 2 \text{ mm}^3$  of a DSTMS bulk single crystal can be obtained by a solution growth method without using a seed crystal. The development of DSTMS has demonstrated that the long-term crystal growth problem hindering development of NLO materials can in principle be solved. A strong effect of intermolecular interactions such as hydrogen bonds on macroscopic non-linearity of stilbazolium salts has been observed. Both the results of powder SHG measurement and crystal growth showed that minor modification of tosylate can induce new stilbazolium derivatives with high SHG efficiencies and improved crystal-growing characteristics.

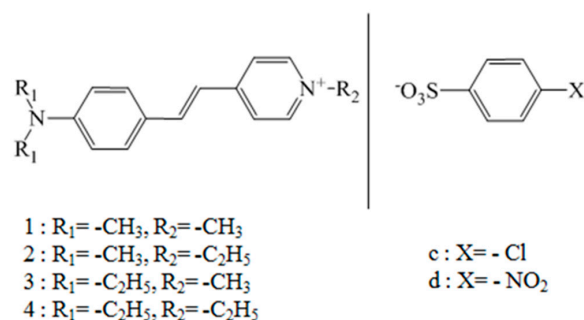


**Figure 2.** Molecule structures of ionic salts synthesized.

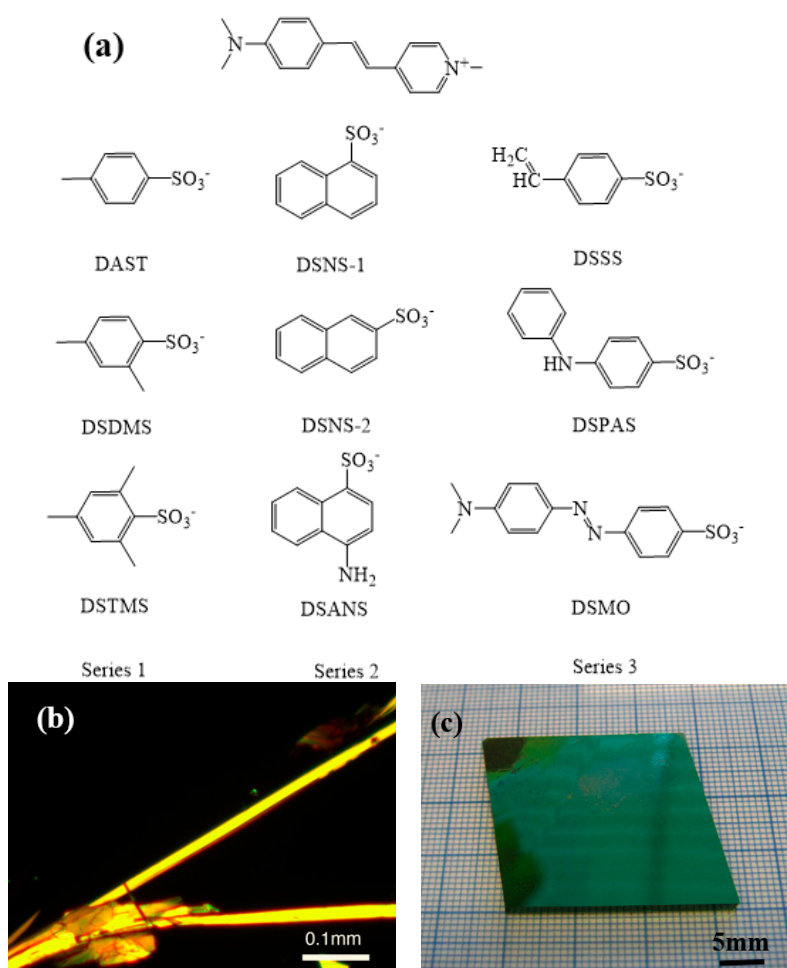


**Figure 3.** Molecule structures of the stilbazolium derivatives (a) and single crystals of 4-*N,N*-dimethylamino-4'-*N'*-methyl-stilbazolium 2-naphthalenesulfonate (DSNS) (b) and 4-*N,N*-dimethylamino-4'-*N'*-methyl-stilbazolium 2,4,6-trimethylbenzenesulfonate (DSTMS) (c).

### 3.2. Design and Change of the Stilbazolium Cation

The benzene of the electron donor and the pyridine of the electron acceptor are ideal combinations for one other in the cation of DAST. So at the beginning of grouping of changes of the DAST cation, most researches were inclined to replace part A and E as mentioned below, while the main channel of electron transport was not changed. The significantly large  $\chi^{(2)}$  values of the above-mentioned ionic organic crystals are due to high  $\beta$  values of stilbazolium cations and due to preferred non-centrosymmetric packing. Generally, the large  $\beta$  values of ionic chromophores are mainly provided by strong electron acceptor and electron donor characteristics of the cation parts. Thus ionic  $\pi$ -conjugated species can be highly polarized when an appropriate substituent is introduced into the cation parts. Therefore, numerous studies on modifying the cation of stilbazolium compounds have been carried out and some interesting achievements have been attained [37–39]. As shown in Figure 4, the cation of DAST could be divided into five parts (A–E). Many research investigations have been concentrated on changing some of the five parts to improve the second order nonlinear property of the cation molecule.

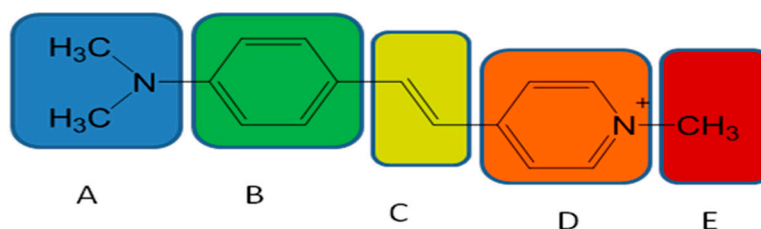


Figure 4. Molecular structure of the modification of DAST cation.

#### Part A

This will be more conducive for the formation of charge transfer system resonances and the broadening of the scope for  $\pi$ -electric charge flow, while the electron-withdrawing/electron-repulsing ability of donor/acceptor becomes stronger. Large  $\beta$  values can be obtained by introducing stronger electron donor and acceptor groups into their molecular structure. Because of a stronger push–pull NLO chromophores enable an efficient charge transfer from the donor to the acceptor upon excitation.

Okada et al. synthesized an organic ion-complex crystal composed of protonated merocyanine and *p*-toluenesulfonate anion, i.e., 1-methyl-4-(2-(4-hydroxyphenyl)vinyl) pyridinium 4-toluenesulfonate (MC-PTS as shown in Figure 5). MC-PTS showed a SHG intensity of 0.14 times as large as that of DAST determined by the powder method at a pumping wavelength of 1064 nm. Single crystal X-ray analysis shows that MC-PTS crystallizes in the space group of P1, in which molecular dipoles are ideally aligned in one direction. It was also indicated that the tetrahedral sulfonate anion plays the part of a chiral handle to cause non-centrosymmetric space groups [40].

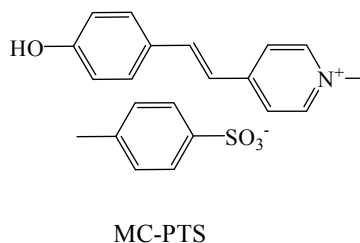
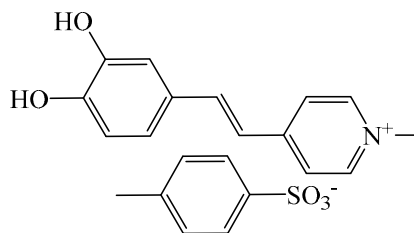


Figure 5. Molecular structure of 1-methyl-4-(2-(4-hydroxyphenyl)vinyl) pyridinium 4-toluenesulfonate (MC-PTS).

The compound 3',4'-dihydroxy-4-*N*-methylstilbazolium tosylate (Figure 6) was prepared by Marder et al. in the early days [41]. A large powder SHG efficiency of 0.1 times of DAST was

observed for this compound. X-ray studies exhibited that this crystallizes in the triclinic space group P1 with one cation and one anion in the unit cell.



**Figure 6.** Molecular structure of 3',4-dihydroxy-4-N-methylstilbazolium tosylate.

As electron donor of the stilbazolium cation, the dimethylamino group  $[-N(CH_3)_2]$  is much stronger than the hydroxyl and dihydroxyl groups, so most of the reported stilbazolium cations possess a dimethylamino group at the position of Part A, for example, DAST, DSNS and DSTMS.

#### Part B

In recent years, it is probable that as many studies found the replacement of part A and E did not produce promising results, following investigations turned to part B and D which play a critical role in nonlinear effects. Research shows that a hetero atom can promote or prevent the pushing/withdrawing effect of a donor/acceptor [42]. Thereby the introduction of heterocyclic rings can improve second-order nonlinearity. It is effective to introduce an aromatic heterocyclic ring with a smaller resonance energy instead of a benzene ring into chromophores, because the higher resonance energy of the benzene ring may easily cause nonlinear susceptibility to reduce or saturate, whereas the different electron density of the aromatic heterocyclic ring can adjust the second-order nonlinear optical susceptibility as an auxiliary to the acceptor [43].

Quantum mechanical studies have suggested that thiophene and pyrrole are more electron-rich heteroaromatic rings than benzene ring [15] series of second-order NLO chromophores with pyrrole and thiophene as (Figure 7) auxiliary electron donors was synthesized by Ma et al. Hyper-Rayleigh scattering measurements at an incident wavelength of 780 nm revealed moderate to very large molecular hypolarizabilities ( $151 \times 10^{-30}$  esu and  $155 \times 10^{-30}$  esu) for chromophores of PPTs and TPTs, respectively. Their magnitude of second-order optical nonlinearities is indicated by a first hyperpolarizability  $\beta$  at the molecular level and a second-order NLO susceptibility ( $\chi^{(2)}$ ) at the molecular integral level [44]. To obtain materials with large  $\chi^{(2)}$ , the optimal combination of both the molecular second-order hyperpolarizability  $\beta$  and the orientation in the bulk are required. In other words, crystals of organic chromophores with large  $\beta$  belonging to non-centrosymmetric space groups are one of the expected forms for bulk materials of large  $\chi^{(2)}$ . However, only a few chromophores with large  $\beta$  have been developed into beneficial bulk crystalline materials for practical NLO applications. This is because most of the chromophores tend to pack in crystals with centrosymmetric space groups which remove all components of  $\chi^{(2)}$ , or although they achieve non-centrosymmetric structures, the  $\beta$  is also direction-sensitive, and the orientation of their molecular dipole moments in the crystalline solid with respect to the polar crystal axes are not optimum for maximizing a second-order NLO response [45].

Li et al. synthesized two series of thienyl-substituted pyridinium salts (Figure 8) with different counter-anions to investigate the effect of the hydrous/anhydrous phase on crystal packing [31]. Single crystals of two kinds of salts (Figure 9) were successfully obtained from methanol by a slow evaporation method. Crystal structure analysis revealed that they crystallized in the monoclinic space group P1 and  $P\bar{1}$ , respectively. TPNS forms a hydrated non-centrosymmetric phase with powder SHG efficiency 0.40 times of DAST at a wavelength of  $\lambda = 2109$  nm. TPDMS gives an anhydrous phase and crystallizes in centrosymmetric structures without a SHG signal. Their study indicated

that thienyl-substituted pyridinium salts tend to crystallize in non-centrosymmetric structure with a hydrous phase [46].

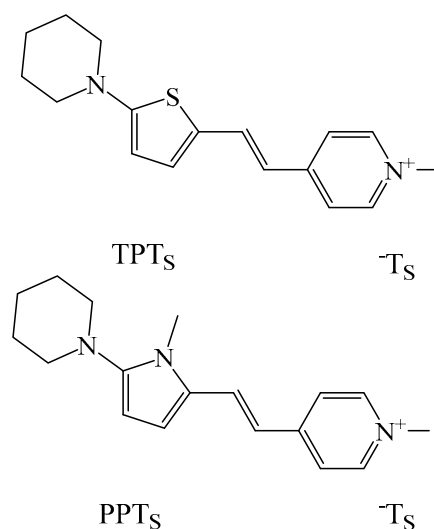


**Figure 7.** Molecular structures of TPTs and PPTs.

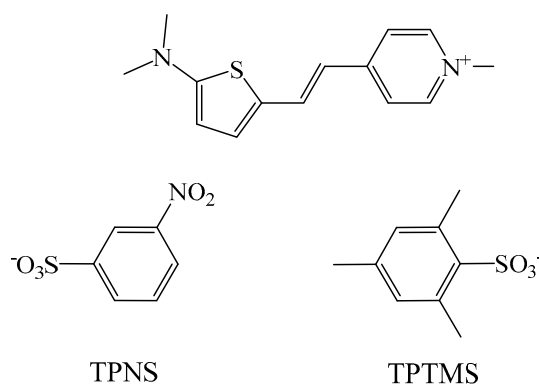


**Figure 8.** Molecular structures of TPNS and TPTMS.

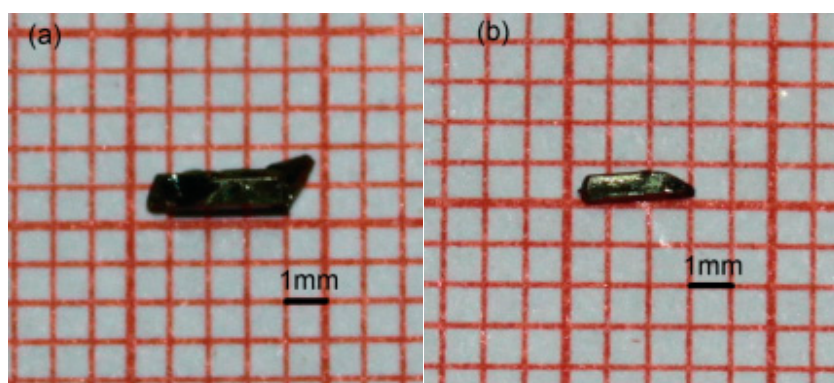


**Figure 9.** Single crystals of TPNS (a) and TPTMS (b).

Tsuji et al. replaced dimethylamino by methoxyl as electron donor and used a naphthalene ring to increase the conjugated system (Figure 10). After sulfonic acid ion replacement, the novel crystal with a large hyperpolarizability  $\beta_0$  of  $870 \times 10^{-30}$  esu was found to give second-order NLO active crystals [47].

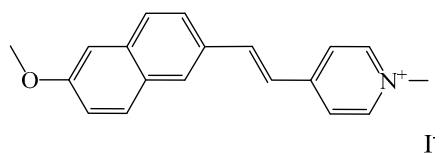


Figure 10. Molecular structure of ionic salts with naphthalene ring.

### Part C

Many research studies have been carried out on introducing different electron delocalization channels into D- $\pi$ -A structures. There are several widely used electron delocalization channels, among them, C=C, C=N, C $\equiv$ C, and N=N (Figure 11) which have been fully studied [34,45]. Different electron delocalization channels have different effects on the nonlinear susceptibility of the molecule. There are two main reasons which lead to the phenomenon of second order polarizability increasing rapidly with growing conjugated chain length: on one hand, the second order susceptibility of the molecules is directly proportional to the square of the length of the conjugated system. On the other hand, steric hindrance between donor and acceptor groups will reduce as the conjugated system elongates.

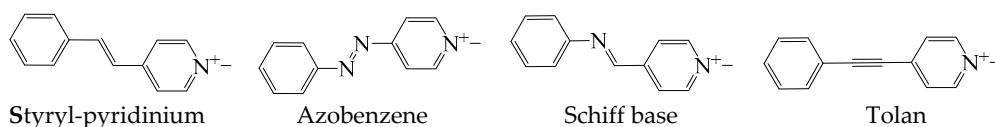


Figure 11. Molecular structures of electron delocalization channels.

#### (1) Styryl-Pyridinium Derivatives

Styryl-pyridinium is one of the most efficient electron delocalized conjugated skeletons. So far most of the reported NLO molecules include this fragment. The carbon and nitrogen atoms on the pyridine ring of styryl-pyridinium are in  $sp_2$  hybrid orbitals, each atom on the ring forms a conjugated system with one  $\pi$  orbital without a lone pair of electrons on the nitrogen atom. Therefore, the formation of stilbazolium does not destroy the cyclic conjugated system. Marder [48] pointed out that the NLO molecule charge transfer mechanism was considered to be achieved by resonance of two limiting forms, ground state and excited state. Second-order molecular polarizabilities tend to be larger as the energies of these two limiting forms are close to each other; such as dimethylamino-styrylpyridinium (Figure 12). The molecules lost aromaticities from conjugated form (i) to conjugate form (ii). However, as first approximation (ignoring the interaction of the corresponding anion), intramolecular charge-transfer is not just as isolated or as neutral molecules. The energy of the two kinds of styryl-pyridinium conjugate forms is close compared with the neutral molecule, which could improve hyperpolarizability  $\beta$  values.

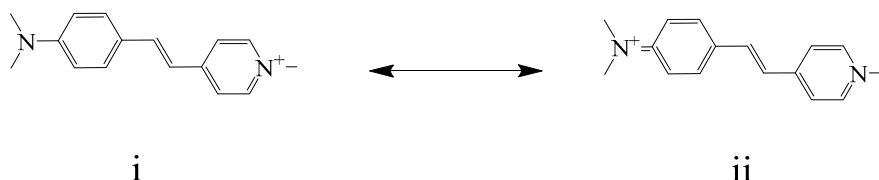


Figure 12. Two kinds of dimethylamino-styrylpyridinium conjugate forms.

#### (2) Azobenzene Derivatives

Azobenzene and its derivatives are characterized by reversible transformations [49] from the generally more stable trans form to the less stable cis form upon irradiation with UV or visible light to yield a photo stationary composition that is wavelength and temperature dependent [50].

Therefore, azobenzene becomes a typical case which demonstrates the property of the N=N double bond. The trans-cis photo isomerization of azobenzene is the basis of photo-responsive properties of many azo-functional materials [51], which produce photochromic [52], photo induced anisotropy, and photo-induced phase transition effects [53]. The isomerization mechanism has drawn extensive attention recently. Many azobenzene derivatives have been developed, including the D- $\pi$ -A neutral molecule [54] and the azobenzene polymer [55] but only rare investigations have focused on the azobenzene ionic species derivatives.

### (3) Schiff Bases

Schiff bases have the ability of intramolecular charge transfer through the entire molecule. In other words, electric charge can be transferred from part D to part A inside D-CH=N-A or A-CH=N-D (D-Donor, A-Acceptor) molecule. From another aspect, styryl-pyridinium derivatives and azobenzene derivatives tend to form planar structures in the solid state, while Schiff bases tend to be non-planar. Two benzene rings twist at a certain angle in the opposite direction along the C1-C $\alpha$  and C1'-C $\alpha'$  bond. That is to say, the conjugation degree of the Schiff base molecule is not equal to other types of molecules, thus the contribution of  $\beta$  value will diminish correspondingly. However, the two benzene rings are not coplanar, which may make the birefringence of the compound not to be too large. Additionally, more importantly, it is because the molecular structure of this kind of plane, symmetry of molecules is reduced, which may give a higher chance of forming a non-centrosymmetric crystal. Meanwhile Schiff bases and their derivatives have a strong frequency multiplication effect and a shorter optical absorption cutoff wavelength, which can improve their transparency [56]. A series of SHG chromophores were designed and synthesized by Coe et al. One of them, as shown in Figure 13, was found to exhibit SHG efficiency 0.43 times of DAST at 1907 nm [57].

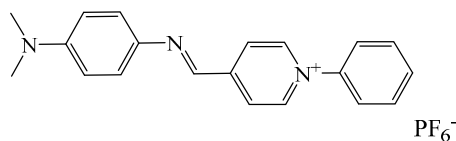


Figure 13. Molecular structure of ionic salt with Schiff base structure.

### (4) Tolan Derivatives

In the case of common organic chromophores, the tolan derivatives were found to have larger NLO properties than a series of stilbene derivatives when compared at the same excitation energy [58]. Since a similar effect was expected for DAST analogues, the ethynyl analogue of DAST and its related compounds with cation 1 (Figure 14) were prepared by Okada et al. and their properties were investigated. Six SHG active salts based on cation 1, including iodide and 4-substituted benzenesulfonates, were found to have non-centrosymmetric structures. The crystal structures of the *p*-chlorobenzenesulfonate salt and *p*-toluenesulfonate salt were analyzed as being isomorphous to one another. As a result, the off-diagonal second-order nonlinear optical coefficient ( $d$ ) values of these two were estimated to be about twice as large as those of DAST [26]. However, tolan derivatives have not been further investigated, perhaps because of the poor thermal and photochemical stability of the ethynyl compared to their ethenyl analogues.



Figure 14. Molecular structure of ionic salt with tolan structure.

### (5) Extension of the Conjugate Chain Length

Tsuji et al. synthesized a series of methoxy stilbazolium analogues (abbreviated as MOSA [1–3]) with  $\pi$ -conjugation extended by attaching a fused aromatic ring, i.e., 6-styrylisoquinolinium

and 4-[2-(2-naphthyl)ethenyl] pyridinium derivatives with methoxy substituents (Figure 15). The experimental  $\beta$  values of MOSA [1,3] at 1064 nm in methanol were evaluated as  $1090 \times 10^{-30}$  esu and  $900 \times 10^{-30}$  esu, respectively. The  $\pi$ -conjugation elongation using fused rings was confirmed to shift the absorption maximum wavelength to shorter wavelengths than in the case of  $\pi$ -conjugation elongation by increasing the double-bond number. This study clarified that the fused-ring systems possess large  $\beta$ , irrespective of their relatively short absorption wavelengths, compared to the double-bond elongation system [33].

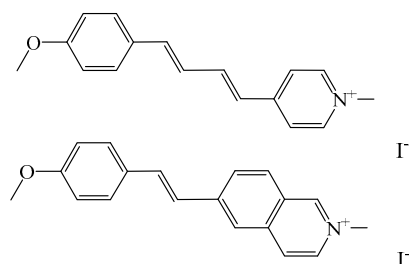


Figure 15. Molecular structures with prolonged conjugate chains.

#### Part D

When introducing other electron acceptors in place of the pyridine ring, it is advantageous to introduce stronger electron withdrawing groups than the pyridine ring. The volume of substitutions in the molecule is another main factor that may improve asymmetry of the compound, resulting in enhancing the possibility of chromophore packing into non-centrosymmetric crystals [59–61].

Chen et al. introduced benzindole to substitute the generally used pyridinium as electron acceptor in the conjugated molecule. Bulk single crystals of P-BI were obtained with sizes of up to  $17.0 \times 6.0 \times 2.0 \text{ mm}^3$  using the slow evaporation method as shown in Figure 16. Kurtz powder tests revealed that the maximum powder SHG efficiency of P-BI with the monoclinic space group  $P2_1$  is 1.14 times the benchmark DAST. Besides, they changed the electron conjugated channel into thiophene. S-BI-1 and S-BI-2 (methanol and ethanol solvent, respectively) were obtained by slow evaporation crystal growth method. The powder SHG efficiency was found to be 0.23 times that of DAST. There is only a small difference in  $\pi$ -conjugation between the molecular structure of P-BI and S-BI but it is accompanied by a large change of molecular ordering in the crystalline state and a substantial change of macroscopic physical properties. These results demonstrate that the crystal packing of this type of salt is very sensitive to the nature of the molecular structure [62].

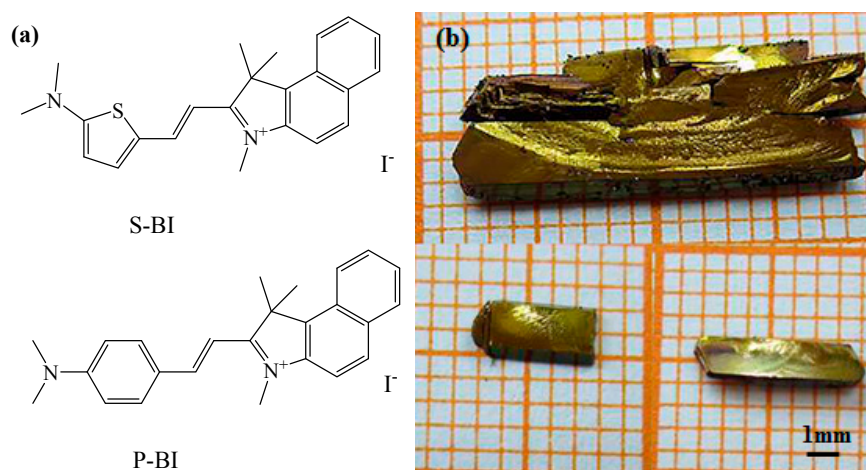
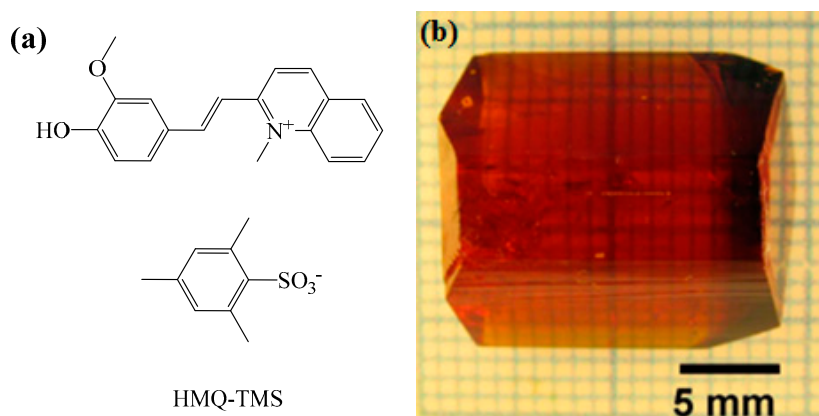


Figure 16. Molecular structures of S-BI and P-BI (a) and single crystals of P-BI (b).

A series of  $\pi$ -conjugated push-pull chromophores was designed and synthesized by Jeong et al., which used various quinolinium derivatives as electron acceptor groups (Figure 17). The same group reported a new organic quinolinium crystal HMQ-TMS which possesses potential for high photoelectricity efficiency and gap-free broadband THz wave generation. It is suitable for the HMQ part to form acentric crystal structures based on Coulomb interactions, therefore a large optical transparency range can be obtained. At the widely used pump wavelength of 800 nm, HMQ-TMS crystals exhibit excellent crystal characteristics, THz generation properties, and offered broader THz spectral coverage [63].



**Figure 17.** Molecular structure of HMQ-TMS (a) and single crystal of HMQ-TMS (b).

A series of quinolinium compounds DA-DMQ1,4-T, DA-DMQ1,2-T and DA-DMQ2,3-T (Figure 18) reveal large macroscopic nonlinear optical response with high hyperpolarizability  $\beta_0$  of 256, 233, and  $122 \times 10^{-30}$  esu, respectively. The electron-withdrawing strength of the derivatives follows the order of DMQ1,2 > DMQ1,4 > DMQ2,3 (Figure 19). The increase of  $\beta_0$  for DA-DMQ1,2-T compared to DA-DMQ2,3-T having the same conjugation length can be explained by the strongly red-shifted wavelength of maximum absorption of the former, caused by the stronger acceptor of 1,2-dimethylquinolinium. The further increase in  $\beta_0$  for DA-DMQ1,4-T over DA-DMQ1,2-T is significant (~10%), but less than might be expected considering the remarkable increase in N-N\* distance alone, which can be attributed to the larger acceptor strength of DMQ1,2 [64].

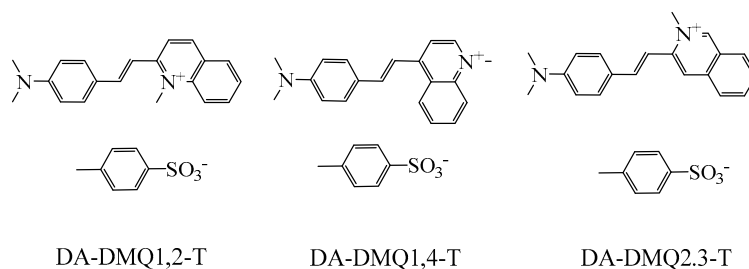


**Figure 18.** Molecular structures of DA-DMQ1,4-T, DA-DMQ1,2-T, and DA-DMQ2,3-T.

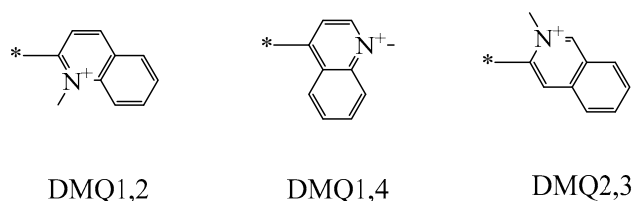


**Figure 19.** Molecular structures of DMQ1,2, DMQ1,4, and DMQ2,3.

Shortly afterwards, new efficient nonlinear optical quinolinium-based single crystals OHQ-TMS were developed by the same group. Remarkably high effective hyperpolarizability tensor values  $\beta_{122}^{\text{eff}}$  of  $27 \times 10^{-30}$  esu were obtained for these crystals. Plate-shaped bulk quinolinium crystals with an area of up to  $56 \text{ mm}^2$  were successfully grown by the solution growth method as shown in Figure 20. The crystal structure of monoclinic acentric space group  $P2_1$  symmetry was obtained by XRD measurement. As-grown OHQ-TMS crystals exhibit a large transparency range from 550 nm to 1600 nm in the optical region and a relatively low absorption coefficient in the THz region. Thus OHQ-TMS crystals are prospective materials for use in second-order NLO applications [65].

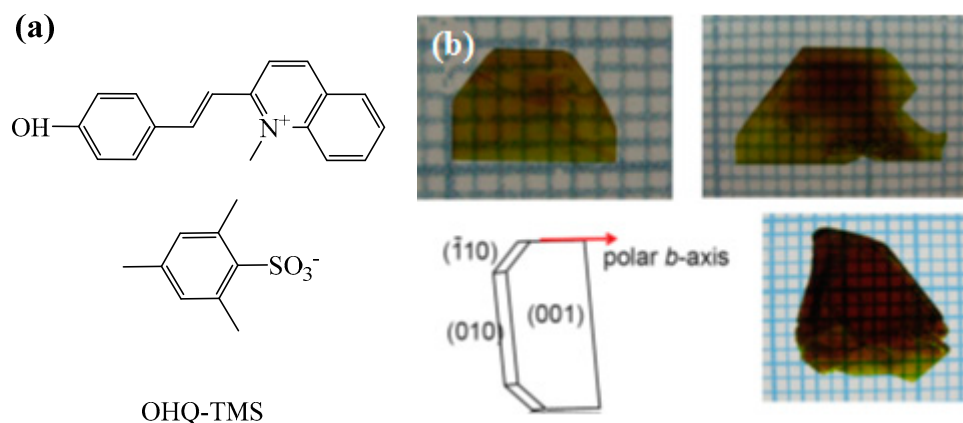


**Figure 20.** Molecular structure of OHQ-TMS (a) and single crystals of OHQ-TMS (b).

#### Part E

For DAST derivatives, it is common to use methyl groups in Part E. Few works have been reported on substitutions of Part E. Coe et al. substituted the methyl by a few other groups. They synthesized a total of sixteen dipolar salts comprising four separate series, each of which includes four different N-substituted pyridinium electron acceptor structures (Figure 21). Almost all of the salts designed crystallize centrosymmetrically, leading to crystals without second-order NLO effects. Fortunately, molecules (6) and (10) adopt the polar space group  $C_C$  and show SHG activity of 0.8 and 1.0 times that of DAST [66,67]. Second-order NLO susceptibility of crystals made of chromophore (6) with  $\text{PF}_6^-$  counter anion higher than that of DAST have been reported [68].

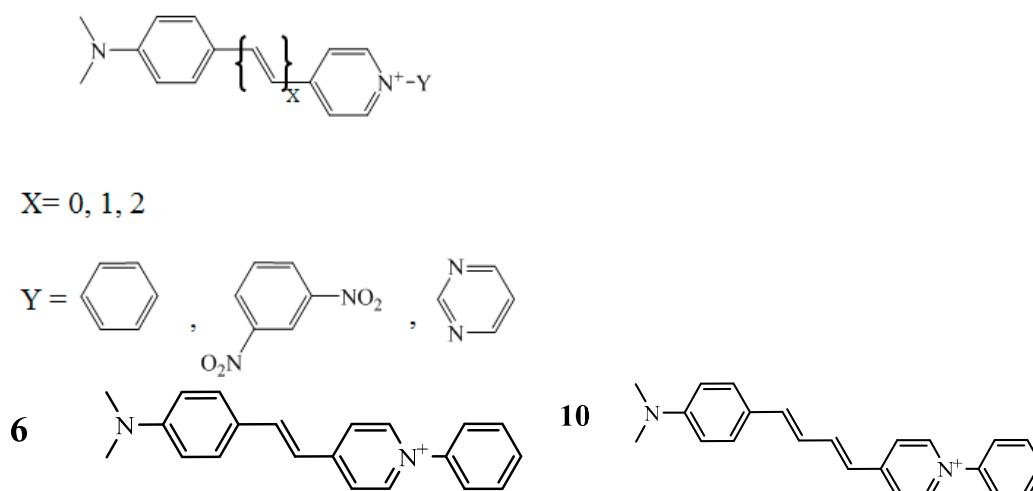


**Figure 21.** Molecular structures with modified Part E.

#### 4. Stilbazolium Dyes in Other Matrices

Although there are a large variety of NLO dyes with high second-order hyperpolarizability  $\beta$  constants have been developed. The principal requirement for SHG is a non-centrosymmetric structure, most of the chromophores have a strong tendency to crystallize centrosymmetrically that leads to a poor SHG effect [69]. Furthermore, novel materials are preferred not only to provide large SHG efficiencies, but also to attribute practical performance such as chemical stability and easy processability for making technological applications [70]. Therefore, researches utilize NLO dyes in other directions such as in self-assembled or multilayers and in polymer NLO dye composite materials. Along this direction, zeolites films and related polymer materials have been proved to be the hosts for aligned inclusion of organic NLO dyes to study novel organic-inorganic composite SHG materials [71].

##### 4.1. Zeolite Films

Zeolites are microporous crystalline aluminosilicates whose solid structure includes channels and cavities at the molecular level. The porosity of the zeolite is open to the exterior and thus it is easy to attract guests inside the lacunae of the zeolite particles. The ability of zeolites to incorporate organic NLO dyes has modified the dyes molecular properties and controlled the interaction with zeolites [72]. Stucky and co-workers gave the first report of the use of inorganic hosts and organic guests to form nonlinear optical materials. According to their study, para-nitroaniline (PNA), 2-methyl-4-nitroaniline (MNA), 2-amino-4-nitropyridine, and analogous compounds are readily introduced into the channels in one direction of  $\text{AlPO}_4\text{-5}$ , and the dye-incorporating  $\text{AlPO}_4\text{-5}$  powders generate a second harmonic with the intensity far exceeding that of quartz powders [73].

##### 4.2. Polymers

Polymers with NLO chromophores are required to be polarized to orient the chromophore in the field direction so that they can attain a macroscopic NLO effect. There are two main forms in which the NLO chromophores and poled polymer could combine together: host-guest polymer system and side-chain polarized polymers system [74]. The host-guest polymer system describes a kind of chromophore-doped polymeric in which the NLO chromophore and micromolecule (guest) can be dissolved in the polymer (host). Though it is quite simple to synthesize this polymeric, the density of the NLO chromophore is limited by the compatibility of host and guest such that the macroscopical NLO coefficient may be more difficult than expected [75]. A side-chain polarized polymers system is a method to make a chromophore bonded to the polymer backbone through a chemical reaction, which can greatly increase the chromophore content that significantly improves the stability of orientation. Besides, some interesting investigations have attempted to use acentric NLO active nanocrystals as building blocks of composite polymers. It has been proven that acentric NLO active nanocrystals can be oriented by a strong directional electric field when dispersed into a liquid host. The orientation process is accompanied by a significant increase of the second harmonic generation which is, however, totally transient due to the high mobility of the dipolar NLO active nanocrystals in the dispersion. Roberto Macchi and coworkers [76] reported that PMMA films containing 4 wt % of DAST obtained by spincoating show in situ growth of homogeneously dispersed oriented nanocrystals with sizes of less than 100 nm. The final film shows a significant and enduring SHG at room temperature.

#### 5. Conclusions

Progress in second-order NLO ionic organic crystal materials has been reviewed. They consist of a positively charged nonlinear optical cation (e.g., stilbazolium) molecule and a negatively charged anion molecule. The cation is the main source of nonlinear optical properties, whereas the counter-anion is used to adjust the crystal packing through coulombic interactions. Variation of counter-ions in organic salts has been confirmed to be an easy and high-efficiency approach for creating crystals

with large second-order NLO activity. It is also effective to improve nonlinear susceptibility of cation molecules by increasing the strength of the donor/acceptor and extending the length of the  $\pi$ -electron conjugated bridge [77,78]. In this paper, the possibilities of modifying the cation chromophores have been discussed and recent examples reviewed.

Many investigations have been conducted to synthesize new organic molecules based on DAST. In the last few years, most of them have tended to change the parts B and D to improve second-order optical nonlinearity of new organic materials and achieve promising goals. It has been found successful to introduce heterocyclic groups such as thiophene and pyrrole into part B. The analogical aromatic furan, which has a similar structure to thiophene is expected to become the focus of future research. In order to develop new organic materials, another polycyclic aromatic hydrocarbon naphthalene with a planar structure just like benzene and larger aromaticity than thiophene is expected to be combined with different part D groups. Moreover, bulk size groups like benzoindoles have been previously considered as not being easy to form non-centrosymmetric crystal packing and are thus inappropriate for introduction into part D. The success of P-BI with 1.14 times SHG efficiency of DAST may draw attention to the modifications in part D with bulk groups.

**Acknowledgments:** This work was supported by the National Natural Science Foundation of China (Grant No. 61370048, 51333001, 51373024, 51473020), the National Key Basic Research Program of China (2014CB931804), the Fundamental Research Funds for the Central Universities (Grant No. FRF-TP-15-003A3).

**Author Contributions:** Xiu Liu collected data and wrote the manuscript. Zhou Yang, Dong Wang and Hui Cao gave suggestion and revised the manuscript.

**Conflicts of Interest:** The authors declare no conflict of interest.

## References

1. Dalton, L.R.; Günter, P.; Jazbinsek, M.; Kwon, O.P.; Sullivan, P.A. *Organic Electro-Optics and Photonics: Molecules, Polymers and Crystals*; Cambridge University Press: Cambridge, UK, 2015.
2. Dalton, L.R.; Sullivan, P.A.; Bale, D.H. Electric Field Poled Organic Electro-optic Materials: State of the Art and Future Prospects. *Chem. Rev.* **2010**, *110*, 25–55. [[CrossRef](#)] [[PubMed](#)]
3. Coe, B.J.; Foxon, S.P.; Helliwell, M.; Rusanova, D.; Brunschwig, B.S.; Clays, K.; Depotter, G.; Nyk, M.; Samoc, M.; Wawrzynczyk, D.; et al. Heptametallic, octupolar nonlinear optical chromophores with six ferrocenyl substituents. *Chem. Eur. J.* **2013**, *19*, 6613–6629. [[CrossRef](#)] [[PubMed](#)]
4. Zheng, Q.D.; He, G.S.; Lin, T.C.; Prasad, P.N. Synthesis and properties of substituted (*p*-aminostyryl)-1-(3-sulfooxypropyl)pyridinium inner salts as a new class of two-photon pumped lasing dyes. *J. Mater. Chem.* **2003**, *13*, 2499–2504. [[CrossRef](#)]
5. Wang, L.; Yu, L.L.; Xiao, X.; Wang, Z.; Yang, P.Y.; He, W.L.; Yang, H. Effects of 1,3,4-oxadiazoles with different rigid cores on the thermal and electro-optical performances of blue phase. *Liq. Cryst.* **2012**, *39*, 629–638. [[CrossRef](#)]
6. Seidler, T.; Stadnicka, K.; Champagne, B. Second-order nonlinear optical susceptibilities and refractive indices of organic crystals from a multiscale numerical simulation approach. *Adv. Opt. Mater.* **2014**, *2*, 1000–1006. [[CrossRef](#)]
7. Marder, S.R.; Perry, J.W.; Schaefer, W.P. Organic salts with large second-order optical nonlinearities. *Chem. Mater.* **1994**, *11*, 37–47. [[CrossRef](#)]
8. Coe, B.J.; Rusanova, D.; Joshi, V.D. Helquat dyes: Helicene-like push–pull systems with large second-order nonlinear optical responses. *J. Org. Chem.* **2016**, *81*, 1912–1920. [[CrossRef](#)] [[PubMed](#)]
9. Coe, B.J.; Foxon, S.P.; Pilkington, R.A.; Sánchez, S.; Whittaker, D.; Clays, K.; Depotter, G.; Brunschwig, B.S. Nonlinear optical chromophores with two ferrocenyl, octamethylferrocenyl, or 4(Diphenylamino)phenyl groups attached to rhenium(I) or zinc(II) Centers. *Organometallics* **2015**, *34*, 1701–1715. [[CrossRef](#)]
10. Matthias, W.K.; Christian, E.; Martin, W.; Stefan, L. Second-Harmonic Generation from Magnetic Metamaterials. *Science* **2006**, *313*, 502–504.
11. Zhuang, S.J.; Teng, B.; Cao, L.F.; Zhong, D.G.; Feng, K.; Shi, Y.X.; Li, Y.N.; Guo, Q.J.; Yang, M.S. The synthesis and purification of 4-dimethylamino-*N*-methyl-4-stilbazolium tosylate. *Adv. Mater. Res.* **2013**, *709*, 36–39. [[CrossRef](#)]

12. Coe, B.J.; Fielden, J.; Foxon, S.P.; Helliwell, M.; Asselberghs, I.; Clays, K.; Mey, K.D.; Brunschwig, B.S. Syntheses and properties of two-dimensional, dicationic nonlinear optical chromophores based on pyrazinyl cores. *J. Org. Chem.* **2010**, *75*, 8550–8563. [[CrossRef](#)] [[PubMed](#)]
13. Kang, S.H.; Jeon, Y.M.; Kim, K.; Houbrechts, S.; Hendrickx, E.; Persoons, A. The diazonium group: An electron acceptor for large molecular hyperpolarizabilities. *J. Chem. Soc. Chem. Commun.* **1995**, *4*, 635–636. [[CrossRef](#)]
14. Rezzonico, D.; Kwon, S.J.; Figi, H.; Kwon, O.P.; Jazbinsek, M.; Günter, P. Photochemical stability of nonlinear optical chromophores in polymeric and crystalline materials. *J. Chem. Phys.* **2008**, *128*, 124713. [[CrossRef](#)] [[PubMed](#)]
15. Wang, L.; He, W.L.; Xiao, X.; Yang, Q.; Li, B.R.; Yang, P.Y.; Yang, H. Wide blue phase range and electro optical performances of liquid crystalline composites doped with thiophene-based mesogens. *J. Mater. Chem.* **2012**, *22*, 2383–2386. [[CrossRef](#)]
16. Li, B.R.; He, W.L.; Wang, L.; Xiao, X.; Yang, H. Effect of lateral fluoro substituents of rodlike cyanomesogens on blue phase temperature ranges. *Soft Matter*. **2013**, *9*, 1172–1177. [[CrossRef](#)]
17. Jazbinsek, M.; Mutter, L.; Günter, P. Photonic applications with the organic nonlinear optical crystal DAST. *IEEE J. Sel. Top. Quantum Electron.* **2008**, *14*, 298–311. [[CrossRef](#)]
18. Pan, F.; Knöpfle, G.; Bosshar, C.; Follonier, S.; Spreiter, R.; Wong, M.S.; Günter, P. Electro-optic properties of the organic salt 4-*N,N*-dimethylamino-4-*N'*-methyl-stilbazoliumtosylate. *Appl. Phys. Lett.* **1996**, *69*, 13–15. [[CrossRef](#)]
19. Dittrich, P.H.; Bartlome, R.; Montemezzani, G.; Günter, P. Femtosecond laser ablation of DAST. *Appl. Surf. Sci.* **2003**, *220*, 88–95. [[CrossRef](#)]
20. Ohma, S.; Takahashi, H.; Taniuchi, T.; Ito, H. Organic nonlinear optical crystal DAST growth and its device applications. *Chem. Phys.* **1999**, *245*, 359–364.
21. Ruiz, B.; Yang, Z.; Gramlich, V.; Jazbinsek, M.; Günter, P. Synthesis and crystal structure of a new stilbazolium salt with large second-order optical nonlinearity. *Mater. Chem.* **2006**, *16*, 2839–2842. [[CrossRef](#)]
22. Umezawa, H.; Tsuji, K.; Okada, S.; Oikawa, H.; Matsuda, H.; Nakanishi, H. Molecular design on substituted DAST derivatives for second-order nonlinear optics. *Opt. Mater.* **2002**, *21*, 75–78. [[CrossRef](#)]
23. Nalwa, H.S.; Miyata, S. (Eds.) *Nonlinear Optics of Organic Molecules and Polymers*; CRC Press: Boca Raton, FL, USA, 1997.
24. Liu, J.L.; Gao, W.; Kityk, I.V.; Liu, X.; Zhen, Z. Optimization of polycyclic electron-donors based on julolidinyl structure in pushpull chromophores for second order NLO effects. *Dyes Pigment.* **2015**, *122*, 74–84. [[CrossRef](#)]
25. Gudar, J.L.; Zyss, J. Structural dependence of nonlinear-optical properties of methyl-(2,4-dinitrophenyl)-aminopropanoate crystals. *Phys. Rev.* **1982**, *26*, 2016–2027.
26. Yin, J.H.; Li, L.; Yang, Z.; Jazbinsek, M.; Tao, X.T.; Günter, P.; Yang, H. A new stilbazolium salt with perfectly aligned chromophores for second-order nonlinear optics: 4-*N,N*-Dimethylamino-4'-*N'*-methyl-stilbazolium 3-carboxy-4 hydroxybenzenesulfonate. *Dyes Pigment.* **2012**, *94*, 120–126. [[CrossRef](#)]
27. Kurtz, S.K.; Perry, T.T. A Powder Technique for the Evaluation of Nonlinear Optical Materials. *J. Appl. Phys.* **1968**, *39*, 3798–3813. [[CrossRef](#)]
28. RajeshKumar, P.C.; Ravindrachary, V.; Janardhana, K.; Poojary, B. Structural and optical properties of a new chalcone single crystal. *J. Cryst. Growth* **2012**, *354*, 182–187. [[CrossRef](#)]
29. Senthil, K.; Kalainathan, S.; Hamadab, F.; Kondo, Y. Bulk crystal growth and nonlinear optical characterization of a stilbazolium derivative crystal: 4-[2-(3,4 dimethoxyphenyl) ethenyl]-1methylpyridinium tetraphenylborate (DSTPB) for NLO device fabrication. *RSC Adv.* **2015**, *5*, 79298–79308. [[CrossRef](#)]
30. Mutter, L.; Brunner, F.D.J.; Yang, Z.; Jazbinsek, M.; Günter, P. Linear and nonlinear optical properties of the organic crystal DSTMS. *J. Opt. Soc. Am. B* **2007**, *24*, 2556–2561. [[CrossRef](#)]
31. Li, L.; Cui, H.J.; Yang, Z.; Tao, X.T.; Lin, X.S.; Ye, N.; Yang, H. Synthesis and characterization of thienyl-substituted pyridinium salts for second-order nonlinear optics. *CrystEngComm* **2012**, *14*, 1031–1037. [[CrossRef](#)]
32. Coe, B.J.; Helliwell, M.; Peers, M.L.; Raftery, J.; Rusanova, D.; Clays, K.; Depotter, G.; Brunschwig, B.S. Synthesis, structures, and optical properties of ruthenium(II) complexes of the tris(1-pyrazolyl)methane ligand. *Inorg. Chem.* **2014**, *53*, 3798–3811. [[CrossRef](#)] [[PubMed](#)]

33. Tsuji, K.; Okada, S.; Oikawa, H.; Matsuda, H.; Nakanishi, H. Styrylpyrylium derivatives for second-order nonlinear optics. *Chem. Lett.* **2001**, *05*, 470–471. [[CrossRef](#)]
34. Yang, Z.; Wörle, M.; Mutter, L.; Jazbinsek, M.; Günter, P. Synthesis, Crystal Structure, and Second-Order Nonlinear Optical Properties of New Stilbazolium Salts. *Cryst. Growth Des.* **2007**, *7*, 83–86. [[CrossRef](#)]
35. Yang, Z.; Aravazhi, S.; Schneider, A.; Seiler, P.; Jazbinsek, M.; Günter, P. Synthesis and Crystal Growth of Stilbazolium Derivatives for Second-Order Nonlinear Optics. *Adv. Funct. Mater.* **2005**, *15*, 1072–1076. [[CrossRef](#)]
36. Brahadeeswaran, S.; Takahashi, Y.; Yoshimura, M. Growth of ultrathin and highly efficient organic nonlinear optical crystal 4'-dimethylamino-N-methyl-4-stilbazolium p-chlorobenzenesulfonate for enhanced terahertz efficiency at higher frequencies. *Cryst. Growth Des.* **2013**, *13*, 415–421. [[CrossRef](#)]
37. Okada, S.; Nogi, K.; Anwar; Tsuji, K.; Duan, X.M.; Oikawa, H.; Matsuda, H.; Nakanishi, H. Ethyl-substituted stilbazolium derivatives for second-order nonlinear optics. *Jpn. J. Appl. Phys.* **2003**, *42*, 668–671. [[CrossRef](#)]
38. Yang, Z.; Jazbinsek, M.; Ruiz, B.; Aravazhi, S.; Gramlich, V.; Günter, P. Molecular engineering of stilbazolium derivatives for second-order nonlinear optics. *Chem. Mater.* **2007**, *19*, 3512–3518. [[CrossRef](#)]
39. Yang, Z.; Mutter, L.; Stillhart, M.; Ruiz, B.; Aravazhi, S.; Jazbinsek, M.; Schneider, A.; Gramlich, V.; Günter, P. Large-Size Bulk and Thin-Film Stilbazolium-Salt Single Crystals for Nonlinear Optics and THz Generation. *Adv. Funct. Mater.* **2007**, *17*, 2018–2023. [[CrossRef](#)]
40. Okada, S.; Masaki, A.; Matsuda, H.; Nakanishi, H.; Kato, M.; Muramatsu, R.; Otsuka, M. Synthesis and crystal structure of a novel organic ion-complex crystal for second-order nonlinear optics. *Jpn. J. Appl. Phys.* **1990**, *29*, 1112–1115. [[CrossRef](#)]
41. Marder, S.R.; Perrya, J.W.; Schaeferb, W.P. 4-N-methylstilbazolium toluene-p-sulfonate salts with large second-order optical non-linearities. *J. Mater. Chem.* **1992**, *2*, 985–986. [[CrossRef](#)]
42. Coe, B.J.; Harris, J.A.; Hall, J.J. Syntheses and quadratic nonlinear optical properties of salts containing benzothiazolium electron-acceptor groups. *Chem. Mater.* **2006**, *18*, 5907–5918. [[CrossRef](#)]
43. Albert, D.L.; Marks, T.J.; Ratner, M.A. Large molecular hyperpolarizabilities quantitative analysis of aromaticity and auxiliary donor acceptor effects. *J. Am. Chem. Soc.* **1997**, *119*, 6575–6582. [[CrossRef](#)]
44. Ma, X.H.; Liang, R.; Yang, F.; Zhao, Z.H.; Zhang, A.X.; Song, N.H.; Zhou, Q.F.; Zhang, J.P. Synthesis and properties of novel second-order NLO chromophores containing pyrrole as an auxiliary electron donor. *J. Mater. Chem.* **2008**, *18*, 1756–1764. [[CrossRef](#)]
45. Okada, S.; Oikawa, H.; Nakanishi, H. Preparation and Crystal Structures of New Colorless 4-Amino-1-methylpyridinium Benzenesulfonate Salts for Second-Order Nonlinear Optics. *Chem. Mater.* **2000**, *12*, 1162–1170.
46. Dai, Y.Q.; Tan, J.F.; Ye, N.; Yang, Z. Synthesis and crystal growth of thienyl-substituted pyridinium derivatives for second-order nonlinear optics. *CrystEngComm* **2014**, *16*, 636–641. [[CrossRef](#)]
47. Tsuji, K.; Nishimura, N.; Duan, X.M.; Okada, S.; Oikawa, H.; Matsuda, H.; Nakanishi, H. Synthesis and properties of novel stilbazolium analogues as second-order nonlinear optical chromophores. *Bull. Chem. Soc. Jpn.* **2005**, *78*, 180–186. [[CrossRef](#)]
48. Marder, S.R.; Beratan, D.N.; Cheng, L.T. Approaches for optimizing the first electronic hyperpolarizability of conjugated organic molecules. *Science* **1991**, *252*, 103–105. [[CrossRef](#)] [[PubMed](#)]
49. Kumar, G.S.; Neckers, D.C. Photochemistry of azobenzene-containing polymers. *Chem. Rev.* **1989**, *89*, 1915–1925. [[CrossRef](#)]
50. Neckers, D.C. *Mechanistic Organic Photochemistry*; Reinhold Pub. Corp.: New York, NY, USA, 1967.
51. Wang, L.X.; Wang, X.G. Progress of the Trans-Cis Isomerization Mechanism of Azobenzene. *Chem. Bull.* **2008**, *4*, 243–248.
52. Yan, X.Z.; Xu, Z.L.; Luo, T.; Yang, P.Q.; Cai, Z.G. The Spectroscopy characteristics and the second-order nonlinear optical properties of novel azobenzene molecules with push-pull structures. *Chem. J. Chin. Univ.* **1997**, *4*, 554–558.
53. Loudwig, S.; Bayley, H. Photoisomerization of an Individual Azobenzene Molecule in Water: An on-off Switch Triggered by Light at a Fixed Wavelength. *J. Am. Chem. Soc.* **2006**, *128*, 12404–12405. [[CrossRef](#)] [[PubMed](#)]
54. Song, X.M.; Feng, Z.C.; Wang, C.Y.; Zeng, H.J.; Liu, L.Y.; Zhan, C.M. Synthesis characterization and photochromic properties of D- $\pi$ -A azobenzene derivatives. *Funct. Mater.* **2015**, *9*, 09114–09119.

55. Zeng, Y.; Pan, Z.H.; Zhao, F.L.; Qin, M.; Zhou, Y.; Wang, C.S. Nonlinear optical properties of an azobenzene polymer. *Chin. Phys. B* **2014**, *23*, 024212. [[CrossRef](#)]
56. Qin, J.G.; Gong, X.P. Relations between structure and nonlinear optical properties of paradisubstitutedbenzaldehyde aniline derivative. *Chin. J. Chem. Phys.* **1991**, *4*, 30–35.
57. Coe, B.J.; Harris, J.A.; Asselberghs, I.; Clays, K.; Olbrechts, G.; Persoons, A.; Hupp, J.T.; Johnson, R.C.; Coles, S.J.; Hursthouse, M.B.; et al. Quadratic Nonlinear Optical Properties of *N*-Aryl Stilbazolium Dyes. *Adv. Funct. Mater.* **2002**, *12*, 110–116. [[CrossRef](#)]
58. Umezawa, H.; Okada, S.; Oikawa, H.; Matsuda, H.; Nakanishi, H. Synthesis and crystal structures of phenylethynylpyridinium derivatives for second-order nonlinear optics. *Bull. Chem. Soc. Jpn.* **2005**, *78*, 344–348. [[CrossRef](#)]
59. Marder, S.R.; Perry, J.W.; Tiemann, B.J. Second-order optical nonlinearities and photostabilities of 2-*N*-methylstilbazolium salts. *Chem. Mater.* **1990**, *2*, 685–690. [[CrossRef](#)]
60. Coe, B.J.; Fielden, J.; Foxon, S.P.; Asselberghs, I.; Clays, K.; Brunschwig, B.S. Two-dimensional, pyrazine-based nonlinear optical chromophores with ruthenium (II) ammine electron donors. *Inorg. Chem.* **2010**, *49*, 10718–10726. [[CrossRef](#)] [[PubMed](#)]
61. Ruiz, B.; Jazbinsek, M.; Günter, P. Crystal growth of DAST. *Cryst. Growth Des.* **2008**, *8*, 4173–4184. [[CrossRef](#)]
62. Chen, H.H.; Ma, Q.; Zhou, Y.Q.; Yang, Z.; Mojca, J.; Bian, Y.Z.H.; Ye, N.; Wang, D.; Cao, H.; He, W.L. Engineering of Organic Chromophores with Large Second-Order Optical Nonlinearity and Superior Crystal Growth Ability. *Cryst. Growth Des.* **2015**, *15*, 5560–5567. [[CrossRef](#)]
63. Jeong, J.H.; Kang, B.J.; Kim, J.S.; Jazbinšek, M.; Lee, S.H.; Lee, S.C.; Baek, I.H.; Yun, H.; Lee, Y.C.; Lee, J.H.; et al. High-Power Broadband Organic THz Generator. *Sci. Rep.* **2013**, *3*, 3200. [[CrossRef](#)] [[PubMed](#)]
64. Jeong, J.H.; Kim, J.S.; Campo, J.; Lee, S.H.; Jeon, W.Y.; Wenseleers, W.; Jazbinsek, M.; Yun, H.; Kwon, O.P. *N*-Methylquinolinium derivatives for photonic applications: Enhancement of electron-withdrawing character beyond that of the widely-used *N*-methylpyridinium. *Dyes Pigment.* **2015**, *113*, 8–17. [[CrossRef](#)]
65. Kim, J.S.; Lee, S.H.; Jazbinsek, M.; Yun, H.; Kime, J.; Lee, Y.S.; Kim, J.W.; Rotermund, F.; Kwon, O.P. New phenolic *N*-methylquinolinium single crystals for second-order nonlinear optics. *Opt. Mater.* **2015**, *45*, 136–140. [[CrossRef](#)]
66. Coe, B.J.; Harris, J.A.; Asselberghs, I.; Wostyn, K.; Clays, K.; Persoons, A.; Brunschwig, B.S.; Coles, S.J.; Gelbrich, T.; Lingt, M.E.; et al. Quadratic Optical Nonlinearities of *N*-Methyl and *N*-Aryl Pyridinium Salts. *Adv. Funct. Mater.* **2003**, *5*, 347–357. [[CrossRef](#)]
67. Coe, B.J.; Harris, J.A.; Clays, K.; Persoons, A.; Wostyn, K.; Brunschwig, B.S. A comparison of the pentaammine (pyridyl) ruthenium (II) and 4-(dimethylamino) phenyl groups as electron donors for quadratic non-linear optics. *Chem. Commun.* **2001**, *10*, 1548–1549. [[CrossRef](#)]
68. Figi, H.; Mutter, L.; Hunziker, C.; Jazbinsek, M.; Günter, P.; Coe, B.J. Extremely large nonresonant second-order nonlinear optical response in crystals of the stilbazolium salt DAPSH. *Opt. Soc. Am. B* **2008**, *25*, 1786–1793. [[CrossRef](#)]
69. Ashwell, G.J.; Hargreaves, R.C.; Baldwin, C.E.; Bahra, G.S.; Brown, C.R. Improved second harmonic generation from Langmuir–Blodgett films of hemicyanine dyes. *Nature* **1992**, *357*, 393–395. [[CrossRef](#)]
70. Tessore, F.; Cariati, E.; Cariati, F.; Roberto, D.; Ugo, R.; Mussini, P.; Zuccaccia, C.; Macchioni, A. The Role of Ion Pairs in the Second-Order NLO Response of 4-*X*-1-Methylpyridinium Salts. *ChemPhysChem* **2010**, *11*, 495–507. [[CrossRef](#)] [[PubMed](#)]
71. Kim, H.S.; Lee, S.M.; Ha, K.; Jung, C.; Lee, Y.J.; Chun, Y.S.; Kim, D.; Rhee, B.K.; Yoon, K.B. Aligned Inclusion of Hemicyanine Dyes into Silica Zeolite Films for Second Harmonic Generation. *J. Am. Chem. Soc.* **2004**, *126*, 673–682. [[CrossRef](#)] [[PubMed](#)]
72. Herance, J.R.; Das, D.; Marquet, J.; Bourdelande, J.L.; García, H. Second harmonic generation of *p*-nitroaniline incorporated on zeolites: Relative efficiencies depending on zeolite structure and film orientation. *Chem. Phys. Lett.* **2004**, *395*, 186–189. [[CrossRef](#)]
73. Cox, S.D.; Gier, T.E.; Stucky, G.D.; Bierled, J. Inclusion Tuning of Nonlinear Optical Materials: Switching the SHG of *p*-Nitroaniline and 2-Methyl-*p*-nitroaniline with Molecular Sieve Hosts. *J. Am. Chem. Soc.* **1988**, *110*, 2987–2988. [[CrossRef](#)]
74. Yitzchaik, S.; Berkovic, G.; Krongauz, V. Charge injection asymmetry: A new route to strong optical nonlinearity in poled polymers. *J. Appl. Phys.* **1991**, *70*, 3949–3951. [[CrossRef](#)]

75. Jiang, W.C.; Pu, H.D.; Li, X.W.; Chen, J.P. The Latest Research Progress of Second-order Nonlinear Optical Polymer. *Polym. Bull.* **2004**, *5*, 28–38.
76. Macchi, R.; Cariati, E.; Marinotto, D.; Roberto, D.; Tordin, E.; Ugo, R.; Bozio, R.; Cozzuol, M.; Pedronb, D.; Mattei, G. Stable SHG from in situ grown oriented nanocrystals of [(E)-N,N-dimethylamino-N'-methylstilbazolium][p-toluenesulfonate] in a PMMA film. *J. Mater. Chem.* **2010**, *20*, 1885–1890. [[CrossRef](#)]
77. Blackburn, O.A.; Coe, B.J.; Helliwell, M.; Raftery, J. Syntheses, structures, and electronic and optical properties of platinum (II) complexes of 1,3-bis(imino)benzene-derived pincer ligands. *Organometallics* **2012**, *31*, 5307–5320. [[CrossRef](#)]
78. Gonzalez-Urbina, L.; Baert, K.; Kolaric, B.; Perez-Moreno, J.; Clays, K. Linear and nonlinear optical properties of colloidal photonic crystals. *Chem. Rev.* **2012**, *112*, 2268–2285. [[CrossRef](#)] [[PubMed](#)]



© 2016 by the authors; licensee MDPI, Basel, Switzerland. This article is an open access article distributed under the terms and conditions of the Creative Commons Attribution (CC-BY) license (<http://creativecommons.org/licenses/by/4.0/>).